International Journal of Nanoelectronics and Materials
*Volume 15 (Special Issue) March 2022* [25-36]

# Waste Mussel Shells as an Adsorbent for Phosphate Removal in Solution: Kinetic and Isotherm Model

Noorul Hudai Abdullah[1*], Slyvester Layang Liom[2], Adam Haqiem Zainudin[2], Muhammad Afiq Irfan Huzil[2], Mohamad Syahrul Syazwan Yaacob[3], Nur Atikah Abdul Salim[4], Masiri Kaamin[1] and Amirreza Talaiekhozani[5]

[1]Neo Environmental Technology, Centre for Diploma Studies, Universiti Tun Hussein Onn Malaysia, Pagoh Education Hub, 84600 Pagoh, Johor, Malaysia
[2]Centre for Diploma Studies, Universiti Tun Hussein Onn Malaysia, Pagoh Education Hub, 84600 Pagoh, Johor, Malaysia
[3]Faculty of Engineering Technology, Universiti Tun Hussein Onn Malaysia, Pagoh Education Hub, 84600, Johor, Malaysia
[4]School of Civil Engineering, Faculty of Engineering, Universiti Teknologi Malaysia, 81310 UTM Johor, Malaysia
[5]Department of Civil Engineering, Jami Institute of Technology, Isfahan, Iran

## ABSTRACT

*Eutrophication occurs when there is excess nutrient, such as phosphates, in water bodies. It causes algae bloom, which in turn disrupts aquatic life. In this study, low-cost waste mussel shell was applied as adsorbent to remove phosphate from aqueous solution ($KH_2PO_4$) by using different adsorbent types and particle sizes. Even though the application of waste mussel shell has been studied before, this study focused on comparing raw and calcined mussel shells with different particle sizes. Waste mussel shells contain high calcium carbonate ($CaCO_3$) and are readily available to be used as an adsorbent to remove phosphates. The study applied pseudo-first-order and pseudo-second-order models for the kinetic model and used Langmuir and Freudlich models for the isotherm model to verify adsorption data with differential equation models. The results show that calcined waste mussel shell adsorbent with a size of 1.18 mm showed the highest phosphate removal (97%). Meanwhile, the best $R^2$ value obtained was 0.999 from the pseudo-second-order model for the 0.075 mm calcined waste mussel shells. The application of waste mussel shells for phosphate removal from solutions can be a significant contribution as an alternative adsorbent in water treatment technologies.*

**Keywords:** Eutrophication, phosphate, waste mussel shells, kinetic model, and isotherm model

## 1. INTRODUCTION

One of the main reasons for the deterioration of water quality in rivers, lakes, and other water sources in most parts of the world is eutrophication, which is caused by human activities [1]. More than 60% of the 90 main lakes in Malaysia have been eutrophicated. Detergent and dish soap water are the most common sources from domestic activity [2] that cause pollution to water sources [3]. Phosphorus in soap water can lead to the growth of algae which consumes oxygen, causing the decrease of oxygen level in the water [4].

Other than that, untreated sewage is released to water bodies in the environment by irresponsible human beings [5] without thinking about the long-term effect on nature [6]. This action can cause eutrophication, which can destroy aquatic life due to the increase of toxins in the water bodies [7].

*noorul@uthm.edu.my

Meanwhile, fertiliser runoff [8] through the water bodies such as ditches contains a lot of phosphorus [9] and nitrogen [10] and can also lead to eutrophication, causing deterioration of oxygen level due to uncontrollable algae growth in the water [11]. As a result, clean drinking water sources become limited in some places, the food chain of animals is disrupted, and many more as all living things cannot survive without water [12].

Calcium carbonate ($CaCO_3$) has the ability to adsorb phosphorus in wastewater [13]. There are a variety of natural sources that contain calcium carbonate such as chalk, snail shells, and mussel shells [14]. Mussel shells are commonly recycled by farmers to increase the pH value of acidic soils in coastal areas [15]. In regions where shellfish aquaculture [16] and canning industries are well established, often in China, Chile, or Spain, mussel shells are an ample residual source of calcium carbonate. Using waste mussel shells as adsorbent can reduce the residual sources [17] which contain calcium carbonate [18] while reducing pollution, because the shells are usually disposed of without proper care [19].

It is a golden opportunity for us to exploit mussel shells because they can be collected for free [20]. Research has been carried out to use waste mussel shells as an adsorbent for phosphate [21] due to potential adsorbent to adsorb phosphate in solutions. The objective of this study is to investigate the removal efficiency of phosphate from aqueous solution using raw and calcined waste mussel shell, evaluate the removal efficiency by different adsorbent types and sizes [22], and determine the adsorption kinetics and isotherm model of phosphorus adsorption onto waste mussel shell.

## 2. MATERIAL AND METHODS

### 2.1 Adsorbent

Two types of adsorbents were used in this research, which are raw and calcined waste mussel shells. To prepare the adsorbent, approximately 2 kg of waste mussel shells was washed with purified water and dried in a drying oven at 30 °C for 2 days [23]. Subsequently, for the calcined sample, the waste mussel shells were calcined in a furnace at 800 °C for 2 h [24]. The shells were crushed and sieved into sizes of 0.075, 0.15, 0.3, 0.6, and 1.18 mm [25].

### 2.2 Synthetic Solutions

An aqueous solution of 10 ppm was prepared by adding 0.1433 g of $KH_2PO_4$ with 1 L of deionised water to make a solution with 100 ppm. The solution was adjusted to 10 ppm by dilution.

### 2.3 Batch Experiment

A volume of 100 mL of synthetic phosphate was mixed with of the raw and calcined adsorbents [26]. For every particle size of the adsorbent, 2 g of the sample was used. Then, the mixture was shaken using an orbital shaker at 170 rpm for 30, 60, 120, 180, 300, 420, 1440, 2880, 4320, and 5760 min. The mixture was then placed into a filtration pump to separate the suspended waste mussel shells, and the phosphate content in the dissolved sample was measured [27].

### 2.4 Analytical Method

HACH DR 6000 UV–vis spectrophotometer was used to determine the phosphorus content using the amino acid method 8178. The sample was sputter-coated (Sputter Coater, Quorum Tech, UK) and subjected to scanning electron microscopy, SEM (COXEM EM-30AX PLUS SEM, Coxem Co, Korea) to determine sample porosity and surface morphology of the adsorbents. EDX instrument (COXEM EM-30AX PLUS SEM, Coxem Co, Korea) was used to determine the chemical composition

of waste mussel shells and the percentage composition of waste mussel shells. Fourier transform infrared (FTIR) spectroscopy (Perkin Elmer Spectrum Two FTIR Spectrometer, USA) was conducted to examine the waste mussel shells before and after phosphorus adsorption. Lastly, XRD instrument (Second Generation BRUKER D2 Phaser Benchtop X-ray Diffraction) was used to determine the crystal phase composition of the adsorbent.

## 2.5 Kinetic Adsorption Model

In adsorption process, adsorption kinetics studies provide information about the sorption mechanism [28], optimum condition, and possible rate-controlling step [29]. Hence, both linear and nonlinear pseudo-first-order and pseudo-second-order models were applied to the adsorption data [30]. During adsorption, there are two processes which are physical and chemical processes [31]. For the physical process, the adsorption is caused by weak attraction forces known as Van der Waals force, while the chemical process occurs when a tight bond forms between the solute and adsorbent, which involves the movement of electrons [32]. Kinetics is calculated by the nature of the adsorbent, solution, and surface flux [33]. The pseudo-first-order and pseudo-second-order models are widely used in almost every adsorption process. Both models depend on the degree of error-correlation coefficient.

### *2.5.1 Pseudo-First-Order Model*

The pseudo-first-order rate equation is commonly expressed as:

$$\ln(q_e - q_t) = \ln(q_e) - k_1 t_i \quad (1)$$

where $q_e$ is the amount of phosphate adsorbed at equilibrium (mg $g^{-1}$), $q_t$ is the amount of phosphate adsorbed at adsorption time (mg $g^{-1}$), $k_1$ is the rate constant of pseudo-first-order equation ($min^{-1}$), and $t_i$ is the adsorption time (min).

### *2.5.2 Pseudo-Second-Order Model*

The pseudo-first-order rate equation is commonly expressed as:

$$\frac{t_i}{q_t} = \frac{1}{k_2 q_e^2} + \frac{t_i}{q_e} \quad (2)$$

where $q_t$ (mg $g^{-1}$) is the amount of phosphate adsorbed at adsorption time, $q_e$ is the amount of phosphate adsorbed at equilibrium (mg $g^{-1}$), $k_2$ is the rate constant of pseudo-second-order model ($min^{-1}$), and $t_i$ is the adsorption time (min).

## 2.6 Isotherm Adsorption Model

Analysis of the isotherm adsorption is important to improve the adsorption process [34]. Linear analysis is widely used in deciding the acceptable fitted adsorption model as it analyses the adsorption process. The best combination for the linear relationship of Freundlich and Langmuir isotherm models needs further analysis of the effects of adsorbent dose on the phosphate removal efficiency.

### *2.6.1 Freundlich Model*

The linear form of the Freundlich isotherm can be written as:

$$ln\, q_e = ln\, K_F + \frac{1}{n} ln\, C_e \quad (3)$$

where $K_F$ is the Freundlich constant (mg $g^{-1}$), $n$ (dimensionless) is the heterogeneity factor which has a lower value for more heterogeneous surfaces, and $C_e$ is the concentration of the adsorbate in the equilibrium solution (mg $L^{-1}$).

### *2.6.2 Langmuir Model*

The linear form of the Langmuir isotherm can be written as:

$$\frac{1}{q_e} = \frac{1}{K_L q_{max} C_e} + \frac{1}{q_{max}} \quad (4)$$

where $q_{max}$ is the maximum adsorption capacity of the adsorbent (mg $g^{-1}$) and $K_L$ is the Langmuir constant (L $mg^{-1}$).

## 3. RESULTS AND DISCUSSION

### 3.1 Physical and Chemical Characteristics of the Waste Mussel Shells

Calcined waste mussel shells were used for this test to determine the physical and chemical properties that allow them to adsorb phosphate effectively [35]. The major chemical compositions of calcined waste mussel shells are Ca (59.74%) and O (38.92%) while the minor compositions are Na (0.60%), Mg (0.06%), K (0.09%), Fe (0.28%), and Sr (0.31%), as shown in Table 1.

**Table 1** Composition of the WMS (wt.%)

| Ca | O | Na | Mg | K | Fe | Sr |
|---|---|---|---|---|---|---|
| 59.74% | 38.92% | 0.60% | 0.06% | 0.09% | 0.28% | 0.31% |

The surface morphology of the calcined waste mussel shells was examined using SEM at magnifications of 1500×, 6000×, and 10000×, as shown in Figure 1. The surface features of calcined waste mussel shells were relatively rough, as shown in Figure 1a and 1b. Calcium oxide occupied the surfaces of the calcined waste mussel shells. The SEM image at 10000× magnification shows small pores on the surface of the calcined waste mussel shells (Figure 1c).

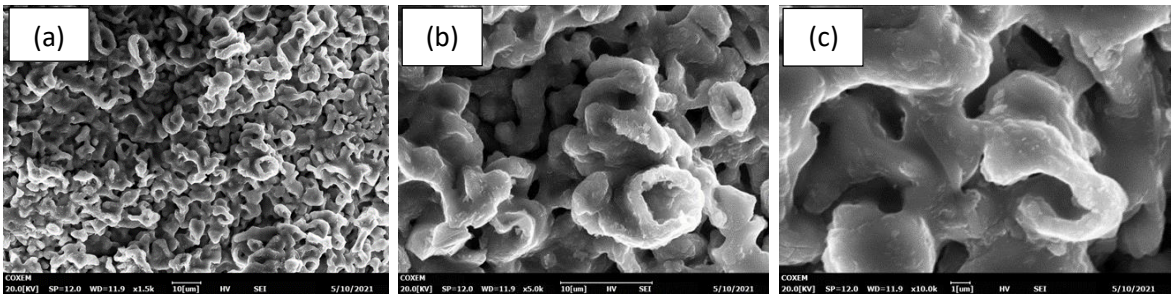


**Figure 1.** SEM photomicrograph of calcined waste mussel shells: (a) 1500× magnification, (b) 6000× magnification, and (c) 10000× magnification.

The FTIR spectra as shown in Figure 2 of natural and $PO_4^{3-}$-adsorbed calcined waste mussel shells were measured and compared over the 400–4000 $cm^{-1}$ range to determine surface functional groups and modifications. Table 2 shows the FTIR spectra of calcined waste mussel shells before and after adsorption of $PO_4^{3-}$ ions. The nature and position of the surface functional groups influence the position and shape of the $PO_4^{3-}$ stretching band in the FTIR spectra of calcined waste mussel shells. The presence of calcium oxide was confirmed by the two bands observed at 713.1

and 873.61 $cm^{-1}$ prior to $PO_4^{3-}$ adsorption. Four bands have a significant shift from their pre-adsorption frequencies of 713.1, 873.61, 1410.29, and 3641.64 $cm^{-1}$. The readings after adsorption were 712.09, 872.48, 1407.71, and 3641.13 $cm^{-1}$.

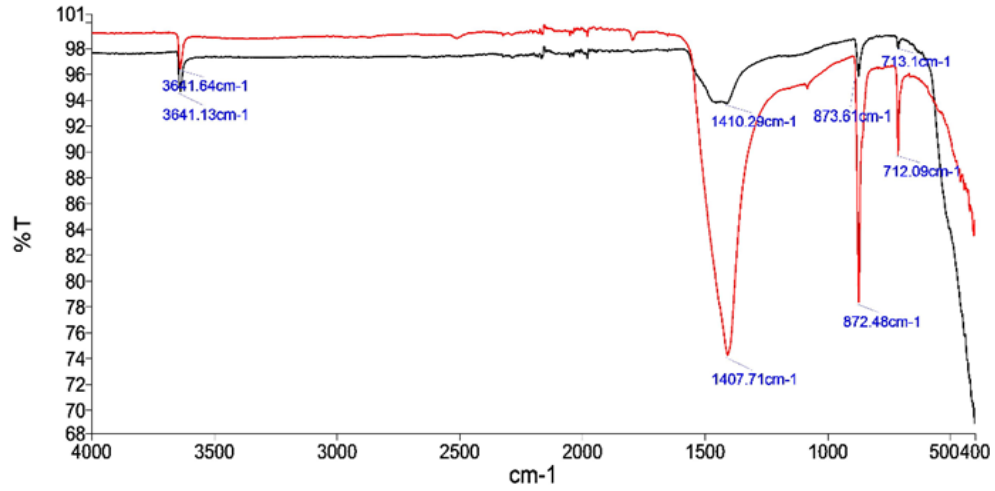


**Figure 2.** The FTIR spectra of WMS of before and after $PO_4^{3-}$ adsorption.

Due to ion exchange between the $PO_4^{3-}$ and C–O functional groups, the influence of $PO_4^{3-}$ molecules adsorbed onto the surface of waste mussel shell on C–O bending increased by 1.01 $cm^{-1}$ (713.1–712.09 $cm^{-1}$) and 1.13 $cm^{-1}$ (872.48–873.61) on the frequency spectrum. Because of the vibrations, this can have an effect on the stretching. The FTIR spectral characteristics of calcined waste mussel shells before and after adsorption of $PO_4^{3-}$ ions are listed in Table 2.

**Table 2** The FTIR Spectral Characteristics of Calcined Waste Mussel Shells Before and After Adsorption of $PO_4^{3-}$ ions

| Frequency spectrum ($cm^{-1}$) | | | Detection of functional group | Reference |
|---|---|---|---|---|
| **Before adsorption** | **After adsorption** | **Difference** | | |
| 3641.13 | 3641.64 | 0.51 | O–H stretching band | [31] |
| 1407.71 | 1410.29 | 2.58 | N–O stretching band | [34] |
| 872.48 | 873.61 | 1.13 | C–O stretching band | [12] |
| 712.09 | 713.1 | 1.01 | C–O stretching band | [28] |

## 3.2 Phosphate Removal Efficiency

In this study, the effectiveness of raw and calcined waste mussel shells in removing phosphate was studied. The results show that using smaller size and longer time for raw waste mussel shells to adsorb phosphate in the wastewater resulted in higher efficiency rate. The results for removal efficiency are shown in Figure 3 and Figure 4 for raw and calcined waste mussel shells, respectively.

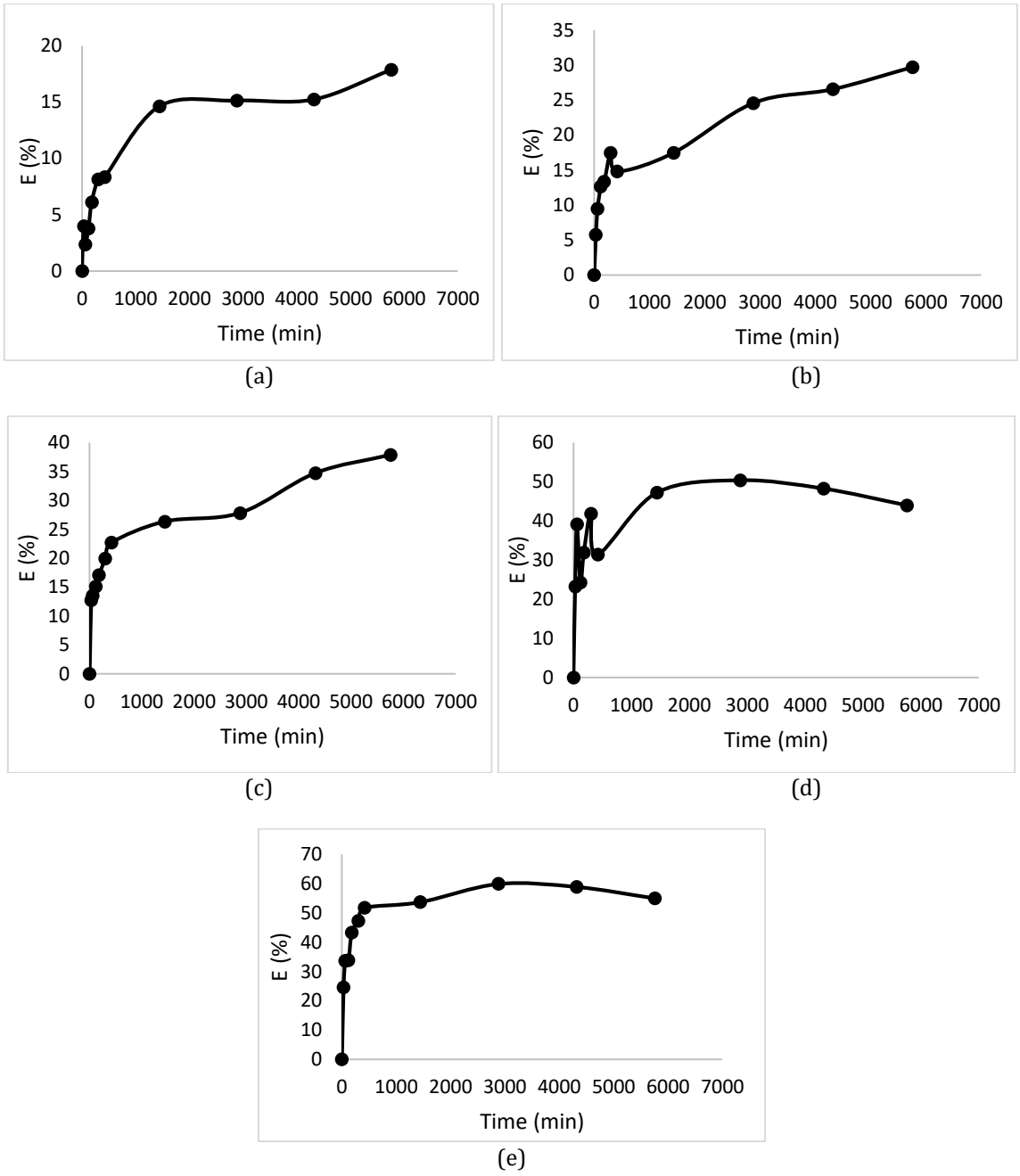


**Figure 3.** Phosphate removal efficiency by using raw waste mussel shells of size (a) 1.18, (b) 0.6, (c) 0.3, (d) 0.15, and (e) 0.075 mm.

Meanwhile, the phosphate removal efficiency using calcined waste mussel shells showed different results. By using adsorbent with sizes of 1.18, 0.6, 0.3, 0.15, and 0.075 mm, the phosphate removal efficiency values were 97%, 96%, 94%, 92%, and 94%, respectively. Calcined waste mussel shells have a better removal efficiency than raw waste mussel shells, where raw waste mussel shell removal efficiency were 15%, 25%, 35%, 47%, and 52%, respectively.

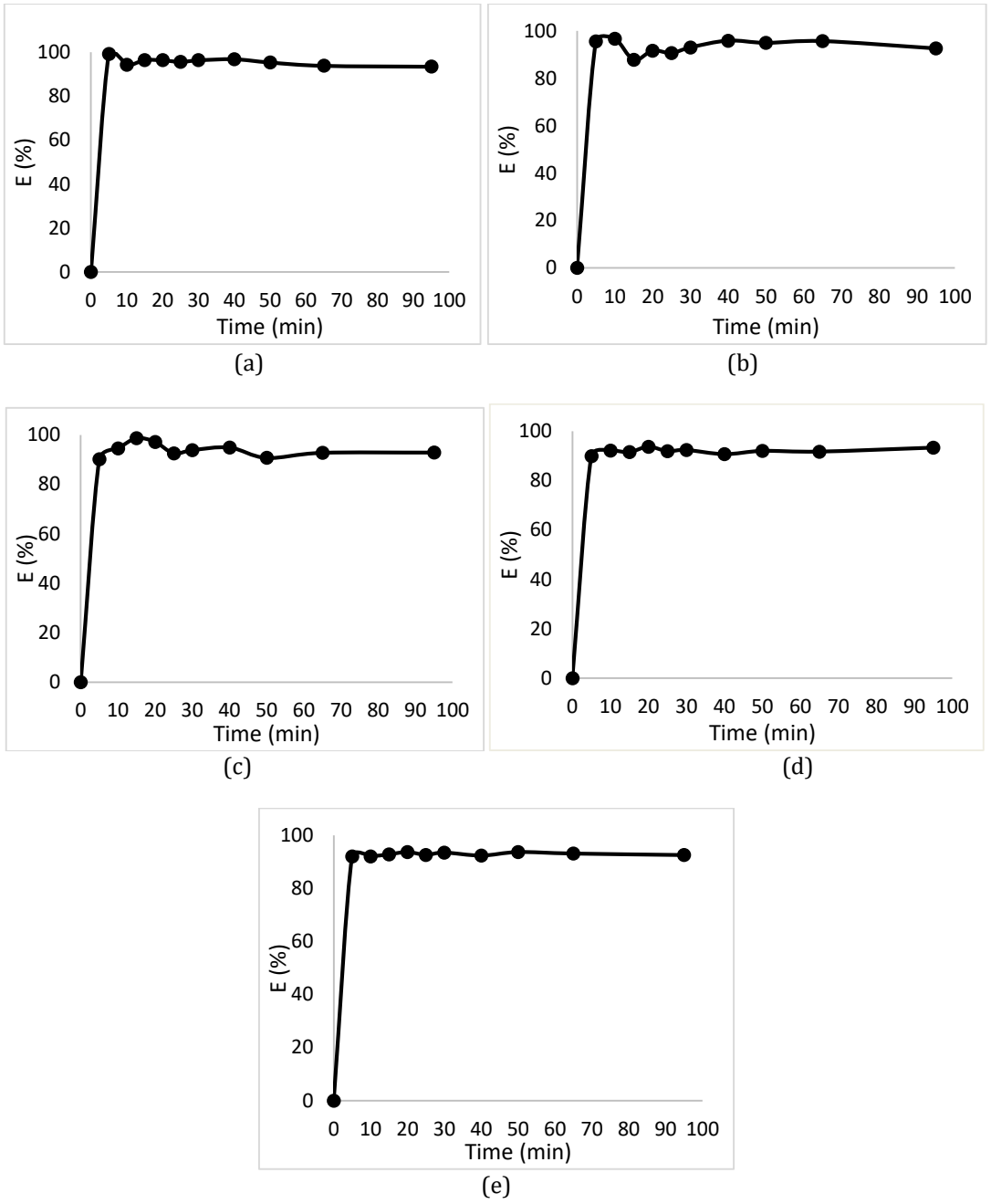


**Figure 4.** Phosphate removal efficiency by using calcined waste mussel shells of size (a) 1.18, (b) 0.6, (c) 0.3, (d) 0.15, and (e) 0.075 mm.

## 3.3 Adsorption Kinetic Model

### *3.3.1 Adsorption of Pseudo-First-Order Model*

Pseudo-first- and pseudo-second-order rate laws are commonly used to model adsorption kinetics [36]. Analyses of published works over the last two decades revealed that the pseudo-second-order model is regarded as the superior model because it can represent a wide range of adsorption systems [37]. The results of using the pseudo-first-order model method are shown in Figure 5.

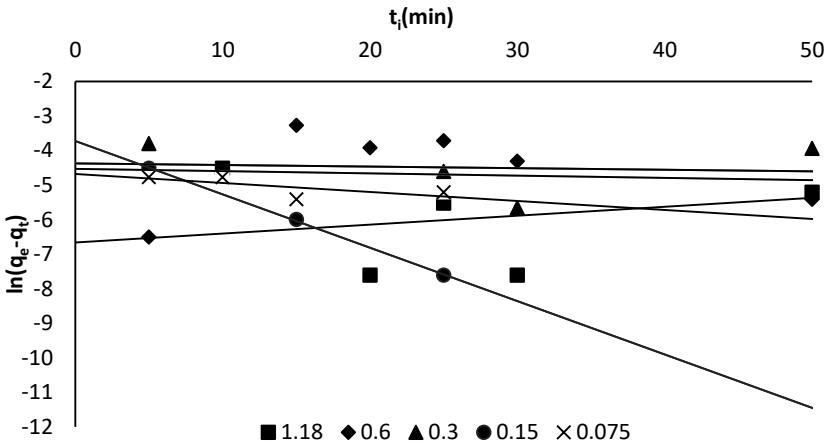


**Figure 5.** Pseudo-first-order graph for calcined waste mussel shell (linear regression analysis for pseudo-first-order model for the adsorption of $PO_4^{3-}$ onto adsorbent from a synthetic solution).

**Table 3** Kinetics Table of Pseudo-First-Order Model (calcined waste mussel shell)

| Pseudo-First-Order | | | | | | |
|---|---|---|---|---|---|---|
| **Sample** | **Particle Size (mm)** | **$q_e$ (theo) (mg g$^{-1}$)** | **$k_2$ (min$^{-1}$)** | **$R^2$** | **$F_e$** | **$q_e$ (exp) (mg g$^{-1}$)** |
| **Synthetic solution** | 1.18–2.36 | 0.0012 | −0.0258 | 0.2768 | 3.2278 | 0.4810 |
| | 0.60–1.18 | 0.0108 | 0.0065 | 0.0213 | 2.4847 | 0.4505 |
| | 0.30–0.60 | 0.0126 | 0.0046 | 0.0482 | 2.7772 | 0.4825 |
| | 0.15–0.30 | 0.0243 | 0.1546 | 0.9994 | 2.6837 | 0.4875 |
| | 0.075–0.15 | 0.0093 | 0.0260 | 0.4824 | 2.8103 | 0.4960 |

Table 3 shows that small adsorbent size is able to adsorb phosphate well with high efficiency [38]. This is shown by the value of $R^2$, which is close to 1, and the lower $F_e$ linear regression analysis. It shows that the adsorbent can adsorb phosphate well in the wastewater. The value of $F_e$ was calculated using Equation 5:

$$F_e = \sqrt{\left(\frac{1}{n-p}\right) \cdot \sum_i^n (q_{t(\exp)} - q_{t(theo)}} \quad (5)$$

### *3.3.2 Adsorption of Pseudo-Second-Order Model*

In a pseudo-second-order reaction, the chemical reaction appears significant in the rate-controlling step. The pseudo-second-order chemical reaction kinetics provided the best correlation for the experimental data, and the adsorption mechanism is chemically rate controlling, which is why it is referred to as chemisorption [38]. The results of using the pseudo-second-order model method are shown in Figure 6.

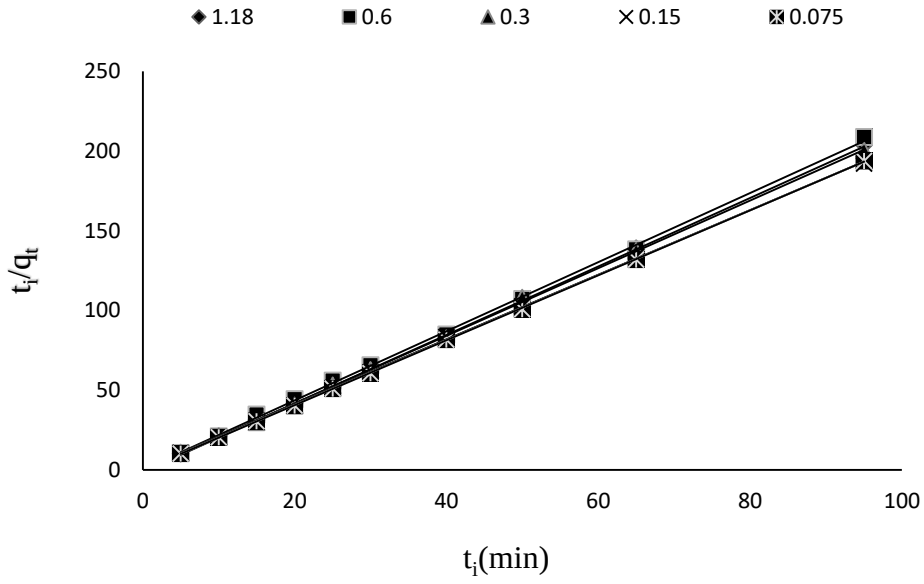


**Figure 6.** Pseudo-second-order graph for calcined waste mussel shell (linear regression analysis for pseudo-second-order model for the adsorption of $PO_4^{3-}$ onto adsorbent from a synthetic solution).

**Table 4** Kinetics Table for Pseudo-Second-Order Model (calcined waste mussel shell)

| Pseudo-Second-Order | | | | | | |
|---|---|---|---|---|---|---|
| **Sample** | **Particle Size (mm)** | **$q_e$ (theo) (mg g$^{-1}$)** | **$k_2$ (g mg$^{-1}$min$^{-1}$)** | **$R^2$** | **$F_e$** | **$q_e$ (exp) (mg g$^{-1}$)** |
| **Synthetic solution** | 1.180–2.360 | 0.4653 | −3.4567 | 0.9998 | 0.05291 | 0.4810 |
| | 0.600–1.180 | 0.4608 | 28.9573 | 0.9992 | 0.06576 | 0.4505 |
| | 0.300–0.600 | 0.4707 | −5.2763 | 0.9995 | 0.07221 | 0.4825 |
| | 0.150–0.300 | 0.4924 | 7.4034 | 0.9998 | 0.02933 | 0.4875 |
| | 0.075–0.150 | 0.4910 | −30.2224 | 0.9999 | 0.02135 | 0.4960 |

Table 4 shows that the adsorbent with the smallest size adsorbed phosphate well with the same high efficiency as the model shown in Table 3. However, what differentiates the pseudo-second-order model and the pseudo-first-order model is the value of $R^2$. Table 4 shows that the adsorbent size of 0.075–0.150 mm has a value of $R^2$ closest to 1 which is 0.9999. This shows that the pseudo-second-order model explains the adsorption better than the pseudo-first-order model.

### 3.4 Adsorption Isotherm Model

In this experiment, the Freundlich and Langmuir models were studied. The Langmuir model assumes a monomolecular layer on the surface at maximum coverage. This means that adsorbed molecules are not stacked. This is not a restriction of the Freundlich isotherm. The Freundlich adsorption isotherm measures the variation in the amount of solution by a unit mass of solid adsorbents as the pressure of a system changes at a given temperature.

**Table 5** Raw Waste Mussel Shells Adsorption Isotherm

| Isotherm Model | Freundlich Model | | | Langmuir Model | | |
|---|---|---|---|---|---|---|
| **Sample** | **n** | **$K_F$ (mg g$^{-1}$)** | **$R^2$** | **$q_{max}$ (mg g$^{-1}$)** | **$K_L$ (L mg$^{-1}$)** | **$R^2$** |
| **Synthetic solution** | −0.37 | 25.91 | 0.95 | 0.04 | −0.21 | 0.80 |

**Table 6** Calcined Waste Mussel Shells Adsorption Isotherm

| Isotherm Model | Freundlich Model | | | Langmuir Model | | |
|---|---|---|---|---|---|---|
| **Sample** | **n** | **$K_F$ (mg g$^{-1}$)** | **$R^2$** | **$q_{max}$ (mg g$^{-1}$)** | **$K_L$ (L mg$^{-1}$)** | **$R^2$** |
| **Synthetic solution** | −10.30 | 0.76 | 0.36 | 1.32 | 2.68 | 0.38 |

Based on Table 5 and Table 6, it can be concluded that the Freundlich and Langmuir isotherm models are the best fit for raw waste mussel shells. The best correlation coefficient, $R^2$ of the Freundlich model is for the raw mussel shells (0.95), which is higher than that of the calcined mussel shell (0.36). Meanwhile, the best correlation coefficient, $R^2$ of the Langmuir model is for the raw mussel shells (0.80), which is greater than that of the calcined mussel shells (0.38). The adsorption of phosphate from the solution occurred on the heterogeneous site with multilayer adsorption, meaning that the adsorbed phosphate on the surface of adsorbent can capture more phosphate.

## 4. CONCLUSION

The batch experiments were conducted to determine the potential for two types of mussel shells (raw and calcined) to remove phosphate from wastewater. The isotherm and kinetic models were verified in this analysis to properly understand the behaviour of phosphate adsorption from synthetic solution onto waste mussel shell adsorbent. The study found that high calcium carbonate content in calcined mussel shells improved phosphate removal. The best particle size for phosphate removal by using calcined waste mussel shells is 1.18 mm because it showed the highest adsorption capacity and removal efficiency (97%). The data fitted best with the pseudo-second-order model, in which the highest correlation coefficient, $R^2$ value (0.999) was obtained for the particle size of 0.075 mm. This indicates that phosphate adsorption occurs by chemisorption. Hence, the calcined waste mussel shell was the good performance in removal efficiency and fitted well with pseudo-second-order model Based on the study, waste mussel shell showed good potential as adsorbents for phosphate removal from wastewater. Phosphate removal using waste mussel shell will be convenient in preventing the water bodies from pollution and eutrophication. It has also proved that this treatment also saves cost as it reuses waste material and is environmentally friendly.

## ACKNOWLEDGEMENTS

This research was supported by the Ministry of Higher Education (MOHE) through Fundamental Research Grant Scheme (FRGS/1/2020/TK0/UTHM/02/22) or Vot No. K308. The authors would also like to thank the Neo Environment Technology (NET), Centre for Diploma Studies (CeDS), Research Management Centre, Universiti Tun Hussein Onn Malaysia for its support.

**REFERENCES**

[1] S. R. Carpenter, "Eutrophication of Aquatic Ecosystems: Bistability and Soil Phosphorus,"in Proc. of the Nat. Aca. of Sci. , United State of America, (2005) pp. 10002–10005.
[2] Zhang M., Pan L., Su C., Liu L., Dou L. Sci Total Environ. vol **1**, issue 758 (2021) pp. 143580.
[3] Feng, Q., Zhang, K., Liu, X., Guan, W., Chen, X., Song, L., Luo, J., Zhaoxia, X., Jiashun, C. J. Wat. Proc. Eng. vol **39,** issue 2020 (2020) pp.101750.
[4] Holly E. G., Tony P., Suyoung C., D. Scott S., Wayne J. P. Wat. Res. vol **182**, issue 2020 (2020) pp. 115968.
[5] Thomas J. W. Met. Finish. vol **100,** issue 1 (2002) pp.781-797.
[6] Song S. L., Shui L. S., Annan Z., Ye S. X. Wat. Res. vol **187,** issue 2020 (2020) pp.116437.
[7] Chislock, M. F., Doster, E., Zitomer, R. A. Wilson, A. E. Nat. Edu. Know. vol **4**, issue 4 (2013) pp.10.
[8] Hong S. H., Akem M. N., Soo C. Y., Chang G. L., Seong J. P. J. Env. Man. vol **270**, issue 2020 (2020) pp. 110817.
[9] Jiaxi J., David I. K., Pema, D., Sherub, P., Seungkwan H., Ho, K. S. Proc. Saf. Env. Pro. vol **126**, issue 2019 (2019) pp.44-52.
[10] Brigita, D., Martins, S., Talis, J., Gunaratna, K. R. Micro. Res. vol **241**, issue 2020 (2020) pp.126586.
[11] Benhong, L., Lei, L., Wei, L. Env. Res. vol **183**, issue 2020 (2020) pp.109218.
[12] Dinka. M. O. Wat. Chall. Urban. Wor. vol **2018** (2018) pp.163-181
[13] N. Z. Kasim, N. A. A. Abd Malek, N. S. Hairul Anuwar, N. H. Hamid, "Adsorptive removal of phosphate from aqueous solution using waste chicken bone and waste cockle shell," in Mat. Today: Proc., United States, (2020) pp.11.
[14] Monneron-Gyurits, M., Joussein, E., Soubrand, M., Fondanèche, P., Rossignol, S. App. Cl. Sci. vol **162**, issue 2018 (2018) pp.15–26.
[15] K. M. Rijaluddin, "Phosphate Removal From Synthetic Wastewater Using Powdered Mussel Shells," in Thesis dissertation, Fac. of Cvil. Eng., Tek. Malaysia Univ., Malaysia, (2018) pp. 1-71.
[16] Martins, M. C., Santos, E. B.H. Marques, C. R. Sci. The Tot. Env. vol **574,** issue 2017 (2017) pp.605–615.
[17] Souza, T.A., Mascarenhas, A.J.S., Andrade, H.M.C., Tereza S. M. Santos. Wat. Air Soil Pollut. vol **229**, issue 2018 (2018) pp.383.
[18] Yirong, C. Vaurs, L. P. J. Env. Chem. Eng. vol 7, issue **6** (2019) pp.103443.
[19] Zulkarnain, A. R. M. B., "Phosphate Removal from Synthetic Wastewater Using Waste Mussel Shells.," in Thesis dissertation. Fac. of Cvil. Eng., Tek. Malaysia Univ., Malaysia, (2018) pp.1-75.
[20] Paradelo, R., Conde-Cid, M., Cutillas-Barreiro, L., Arias-Estévez, M., Nóvoa-Muñoz, J.C., Álvarez-Rodríguez, E., Fernández-Sanjurjo, M.J., Núñez-Delgado, A. Ecol. Eng. vol **97**, issue 2016)pp.558–66.
[21] Abdul Salim, N., Mohd, P., Abdull Rahim, M. Y., Abdullah, N. H., Fulazzaky, M. A., Mohd, A., Mohd Hairul, K., Ahmad Zaini, M. A., Syafiuddin, A., Ahmad, N., Mat Lazim, Z., Nuid, M. Zainuddin, N. Malay. J. Fund. App. Sci. vol **16**, issue 3 (2020) pp.393-399.
[22] Liu, D., Zhu, H., Wu, K., Wang, F., Zhao, X., Liao, Q. Cons. Buil. Mat. vol **236,** issue 2020 (2020) pp.117526.
[23] Wadood, T. M. Sarmad, A. R. Inter. J. Chem. Eng. vol **2012** (2012) pp.125296.
[24] Köse, T. E. Köse, T. E., Kıvanç, B. Chem. Eng. J. vol **178,** issue 2011 (2011) pp.34–39.
[25] Sidra, I., Deepika L. R., Varsha, S., Muhammad, B. A., Mika, S. Chemosphere. vol **204**, issue 1018 (2018) pp.413–430.
[26] Wei, J., Ge, J., Rouff, A. A. Wen, X., Meng, X., Song, Y. J. Env. Chem. Eng. vol.**7**, issue 5 (2019) pp.103334.
[27] Henze, M. Wat. Sci. Tech. vol **35**, issue 10 (1997) pp.1–4.

[28] Sari, A. A., Amriani, F., Muryanto, M., Triwulandari, E., Sudiyani, Y., Barlianti, V., Lotulung, P. D. N., Hadibarata, T. J. Taiw. Inst. Chem. Eng. vol 77, issue 2017 (2017) pp.236–243.
[29] Johir, M.A.H., Pradhan, M., Loganathan, P., Kandasamy, J., Vigneswaran, S. J. Env. Manage. vol **167**, issue 2016 (2016) pp.167–174.
[30] Ezzati, R. Chem. Eng. J. vol **392,** issue 2020 (2020) pp.123705.
[31] Fan, L., Brett, M. T., Li, B. Sci. Tot. Env. vol **721**, issue 2020 (2020) pp.1–8.
[32] Shamkhi, M. S. Wasit J. Sci. and Med. vol **4** (2019) pp.1–11.
[33] Guo, X., Wang, J. J. Mol. Liq. vol **288**, issue 2019 (2019) pp.111100.
[34] De-Bashan, L. E., Bashan, Y. Wat. Res. vol **38**, issue 19(2004) pp.4222–4246.
[35] Agarwal, S., Rani, A. J. Env. Chem. Eng. vol **5**, issue 1 (2017) pp.526–538.
[36] Guo, X., Wang, J. J. Mole. Liq. vol **296**, issue 2019 (2019) pp.111850.
[37] Liguo, Z., Jingshi, P., Lei, L., Kang, S., Qilin, W. J. Clean. Prod. vol **238**, issue 2019 (2019) pp.117904.
[38] Wu, F. C., Tseng, R. L., Huang, S. C., Juang, R. S. Chem. Eng. Jour. vol **151**, issue 1 (2009) pp.1–9.